ICANS-XIV
14th Meeting of the International Collaboration on
Advanced Neutron Sources
June 14-19, 1998
Starved Rock Lodge
Utica, Illinois

Performance of the Small-Angle Diffractometer SAND at IPNS[#]

P. Thiyagarajan, V. Urban, K. Littrell, C. Ku, D.G. Wozniak, H. Belch, R. Vitt,
J. Toeller, D. Leach, J.R. Haumann, G.E. Ostrowski, L.I. Donley, J. Hammonds,
J.M. Carpenter and R. K. Crawford
Argonne National Laboratory, Argonne, IL 60439, USA.

ABSTRACT

The time-of-flight small-angle diffractometer SAND has been serving the scientific user community since 1996. One notable feature of SAND is its capability to measure the scattered intensity in a wide Q ($4\pi\sin\theta/\lambda$, where 2θ is the scattering angle and λ is the wavelength of the neutrons) range of 0.0035 to 0.5 $Å^{-1}$ in a single measurement. The optical alignment system makes it easy to set up the instrument and the sample. The cryogenically cooled MgO filter reduces the fast neutrons over two orders of magnitude, while still transmitting over 70% of the cold neutrons. A drum chopper running at 15 Hz suppresses the delayed neutron background. SAND has a variety of ancillary equipment to control the sample environment. In this paper we describe the features of the SAND instrument, compare its data on a few standard samples with those measured at well established centers in the world, and display two scientific examples which take advantage of measuring data in a wide Q-range in a single measurement. With a new set of tight collimators the Q_{min} can be lowered to 0.002 $Å^{-1}$ and the presently installed high-angle bank of detectors will extend the Q_{max} to 2 $Å^{-1}$.

1. Introduction

Small angle neutron scattering (SANS) is a general purpose nondestructive technique that enables the structural study of systems in nanometer to submicron length scale. When dealing with systems that undergo changes such as aggregation, phase transition or gelation as a function of time, it is essential to obtain the scattering data in a wide Q-range all at once. At reactor-based SANS instruments the range is spanned by making repetitive measurements in different instrument configurations and wavelengths. This

[#] Work supported by U.S. Department of Energy, BES, Contract No. W-31-109-ENG-38.
Keywords: Small-angle, Instrument, performance.

becomes cumbersome and at times a great challenge to the scientists dealing with systems which may be either very delicate or very difficult for exact reproduction of both the sample and its environment in order to repeat the experiments. TOF-SANS instruments at pulsed sources are more effective for the study of such systems as they produce data in a wide Q-range in a single measurement.

The SAND instrument was designed based on over 10 years experience of running the SAD instrument [1] at IPNS for the scientific user community. The main objectives were to extend the Q-range of SAND beyond that of SAD (0.005 to 0.25 $Å^{-1}$), increase ΔQ resolution and intensity, and improve ease of operation. The design aspects of SAND have been already published [2]. We have published the physics assessment of cryogenically cooled MgO crystals as a neutron filter [3] and a theoretical discussion of the design and use of a drum chopper for reducing the delayed neutron background and extending the usable wavelength range by the elimination of alternate frames [4]. The data reduction procedure used at SAND is exactly the same as that for the SAD instrument [1].

2. Overview

Here we give an overview of the present features of SAND and its performance. The SAND instrument was designed to measure data in a Q-range of 0.002 to 2 $Å^{-1}$ in a single measurement. In the present configuration SAND enables measurements in a Q region of 0.0035 to 0.5 A^{-1} and we anticipate that it will reach its design goal in the near future. The minimum and maximum Q values to be reached are

$$Q_{min}=2\pi\phi_{min}/\lambda_{max} \qquad (1)$$

$$Q_{max}=2\pi\phi_{max}/\lambda_{min} \qquad (2)$$

In order to reach the smallest Q_{min} the SANS has to be measured at the lowest angle (ϕ_{min}) using neutrons with longest wavelength (λ_{max}). Similarly, the largest Q_{max} is accomplished by measuring data at the largest angle (ϕ_{max}) using the shortest wavelength (λ_{min}).

Fig.1 depicts the SAND instrument schematic and Table I presents the relevant instrument parameters. SAND has the same length as SAD and views the same cold source. However, it has a larger sample-to-detector distance, an optical alignment system, a larger area detector, a high-angle detector bank, a chopper to reduce the delayed neutron background, a better cryogenic cooler for the MgO filter, and a number of upgrades to control the sample environment.

At IPNS neutrons in 30 Hz pulses are produced by spallation in a depleted uranium target by 450 MeV protons (0.3 μsec duration) with a time-averaged proton current of 15 μA. A solid methane moderator at 24 K in a 0.7 l aluminum container grooved on the viewed side to increase the cold neutron flux thermalises high-energy neutrons. This moderator has been designed to maximize the cold neutron flux while preserving a narrow pulse width at each wavelength. Graphite and beryllium reflectors decoupled by a 0.5 mm layer of cadmium surround the moderator. Significant fast neutrons and γ-rays exist in the

prompt beam spectrum, and if not attenuated cause detector recovery effects that can persist to long times-of-flight.

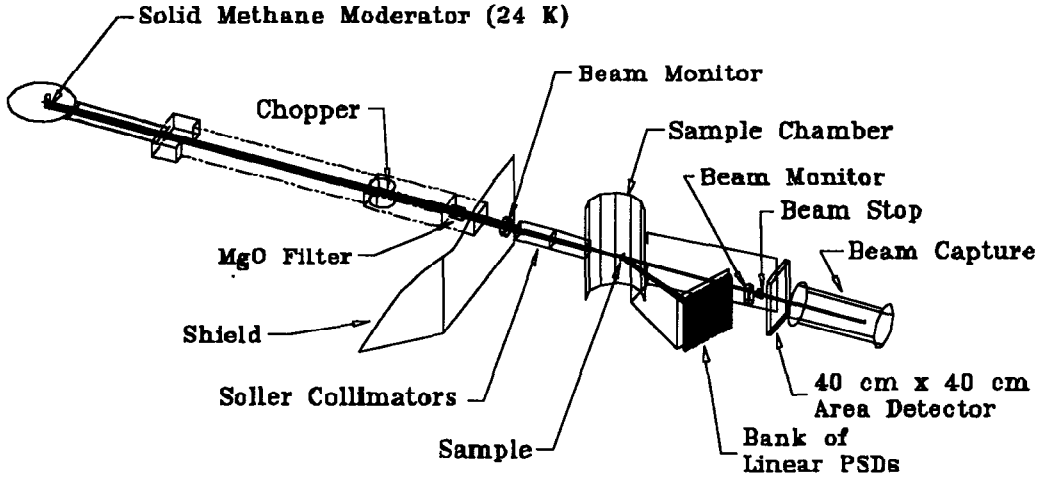

Figure 1. Schematic of TOF-SANS instrument, SAND at IPNS.

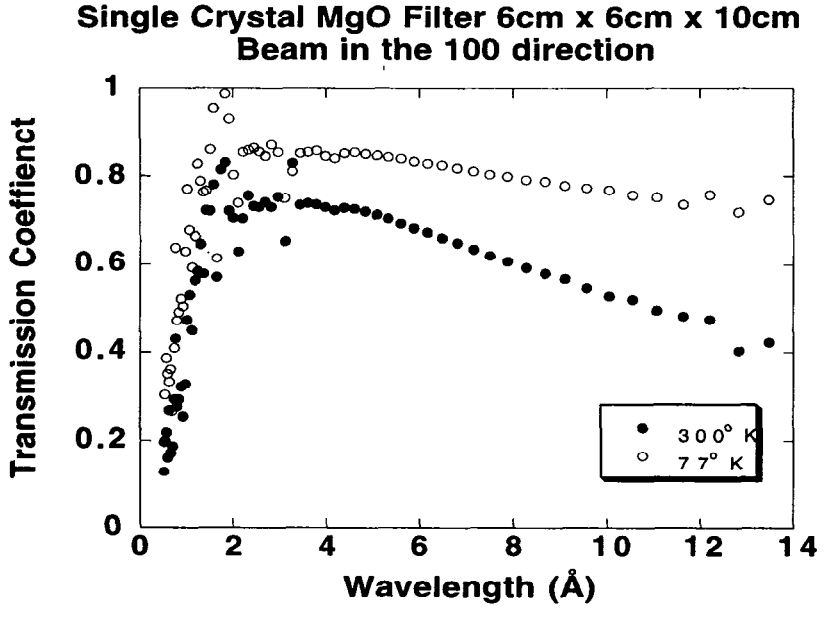

Figure 2. Measured Transmission coefficients of MgO filter.

Table 1. Instrument Parameters of SAND

Parameter	Value
Source frequency	30 Hz
Moderator	decoupled Solid CH_4 at 24 K
Source-to-sample distance	7.00 m
Source-to-beam monitor (M1)	5.65 m
Source-to-Transmitted beam monitor(M2)	8.65 m
Sample-to-area detector distance	2.00 m
Sample-to-LPSD distance	1.524 m
Focusing collimators	
Coarse	0.0034 radians fwhm
Fine	0.0014 radians fwhm
Vertical focusing collimator	
Entrance width / channel	0.1 cm
exit width / channel	0.0894 cm
Collimator exit-sample distance	77 cm
length	32.8 cm
Horizontal focusing collimator	
Entrance width / channel	0.0844 cm
exit width / channel	0.0767 cm
Collimator exit-sample distance	50 cm
length	25 cm
Beam diameter at moderator	9.0 cm
Maximum Beam diameter at sample	2.0 cm
Beam diameter at area detector	2.1 cm
Area detector	
active volume	40 x 40 cm^2, 2.5 cm thick
Fill gas	2.6 atm ^3He & 0.8 atm (95% Xe+5% CO_2)
Resolution	6-8 mm fwhm
Encoding	rise time, 128 x 128 pixels
max scattering angle	9°
LPSD	
active volume per detector	1.1 cm dia x 60 cm long
number of detectors	65
resolution	1-2 cm along detector
fill gas	~6 atm ^3He
encoding	charge division, 64 segments / detector
max scattering angle	36°
Wavelength range	0.5 - 14 Å (68 channels const $\Delta T/T=0.05$)
$\mathbf{Q_{max}}$	2 $Å^{-1}$

A cryogenically cooled (77 K) MgO filter arranged to have a cross section of 6 cm x 6 cm and a length of 10 cm is employed as a filter. This consists of 27 crystals of dimensions 2 cm x 2 cm x 2 cm and 32 crystals of dimensions 1.5 cm x 1.5 cm x 2 cm.

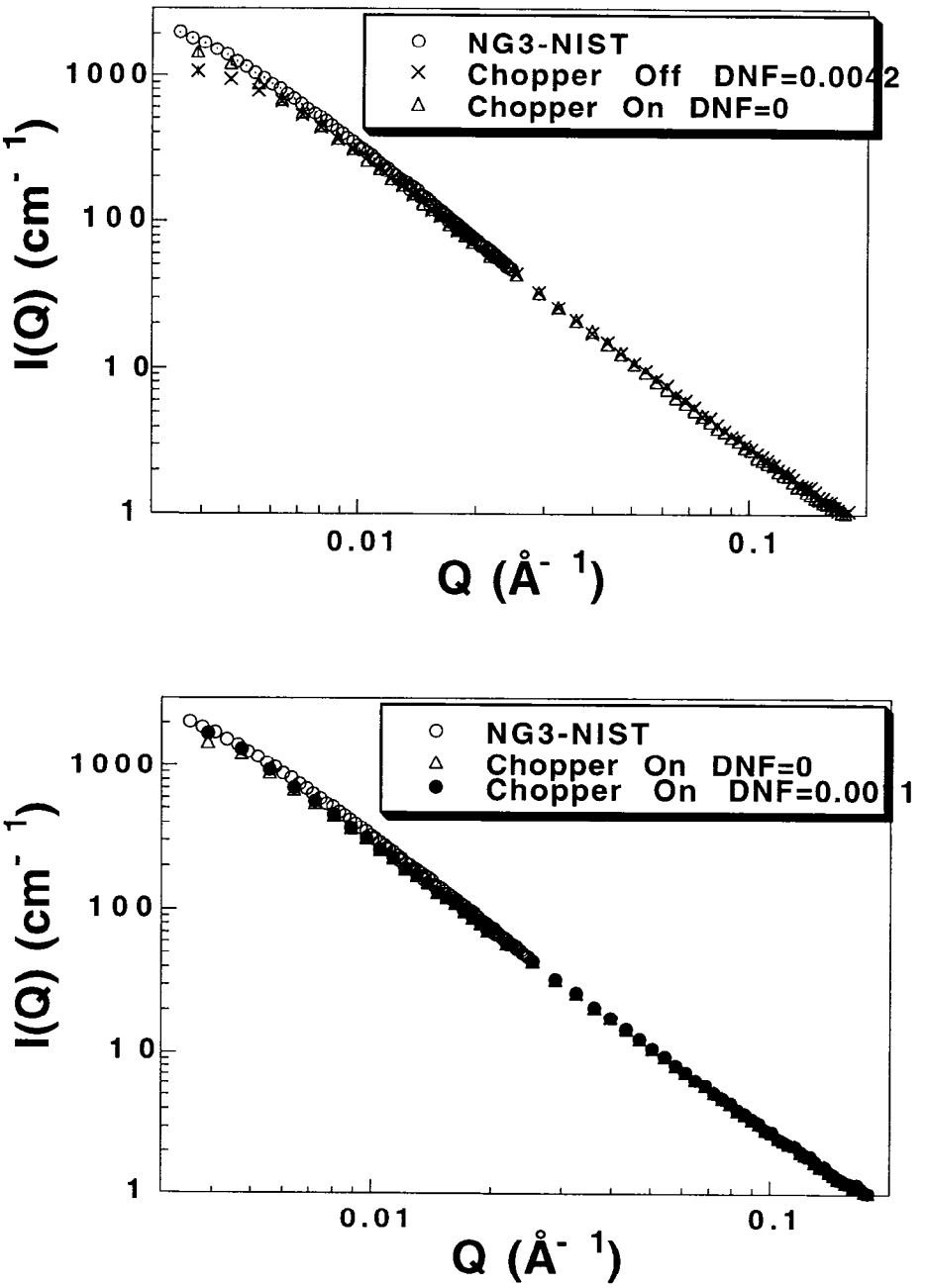

Figure 3. Comparison of the low Q data of Bates-poly with and without the Delayed Neutron Chopper.

We recently showed that MgO is the best choice for attenuating the fast neutrons while still achieving the best transmission of cold neutrons [3]. The measured transmission coefficients of this filter at ambient and 77 K are shown in Fig. 2. The use of the MgO filter, however, limits the usable λ_{min} to 1 Å.

The depleted uranium target produces delayed neutrons that arrive at the detector at all times. This produces a sample-dependent background that has to be corrected [5]. The effects due to delayed neutrons are very high for the samples rich in hydrogen. One can employ software techniques [1,5] to correct for the effects due to delayed neutrons. However, a chopper can nearly eliminate the background coming into the long wavelength channels that produce data in the low Q region. We have shown that a ~ 18.5 cm diameter drum chopper with a ~ 1 cm thick B_4C shell as the absorber, operated at 15 Hz (open twice per revolution) can serve this function [4]. Reducing the background by the chopper produces higher quality data in the low Q region than just the software correction. This is illustrated in Fig. 3 where we compare the data for the Bates-poly standard with the measured absolute differential scattering cross-section at the NG3-SANS at NIST. It is clearly seen that the SAND data measured with the chopper with no correction agrees better with the NIST data than that corrected by using just the software. Using software correction for the residual delayed neutrons further improves agreement.

The usable λ_{max} at SAND is restricted to 14 Å by the source frequency of 30 Hz at IPNS and the 9 m the source-to-detector distance. Currently, SAND produces data in the Q region of 0.0035 to 0.5 $Å^{-1}$. This already surpasses the Q-range and the quality of the data produced by SAD. The SANS data for the Bates-poly standard measured at SAD and SAND for 30 minutes are shown in Fig. 4. It is clearly seen that the data from SAND extends both ends of the Q-range of SAD. Furthermore, the statistical precision of the SAND data is higher than that of SAD in a Q region of 0.08 to 0.25 $Å^{-1}$.

The background in the low Q region is higher at SAND than that at SAD. Since this effectively limits the Q_{min} for the weak scatterers, systematic investigations are underway to determine the source of this background. Even though this background differs from the anisotropic background produced by the previously used Soller collimators at SAD [6], we cannot rule out Soller collimators at SAND as a source.

We plan to extend this lower Q_{min} value by increasing the λ_{max} of the neutrons and tightening the collimation. Since the solid methane moderator produces a significant flux of long wavelength neutrons, the chopper can be used as a frame-elimination chopper [4]

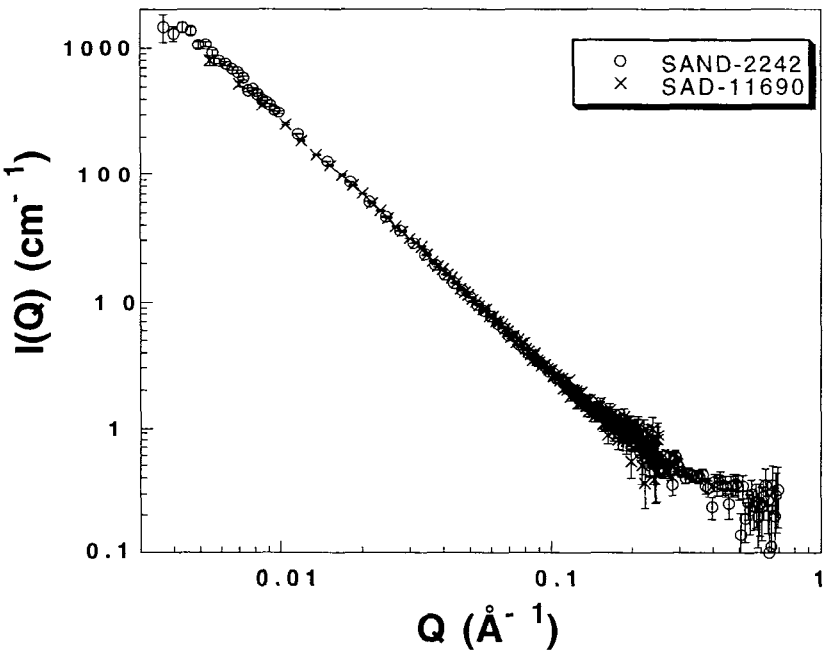

Figure 4. Comparison of SANS data for Bates-poly measured at SAD and SAND.

to extend the λ_{max} at SAND. As neutrons of different wavelengths travel with different velocities, the short-wavelength neutrons arising from one source pulse can arrive at the detector at the same time as the slower, long wavelength arising from a previous pulse. This overlap of neutron pulses in the detector, known as frame overlap, imposes an effective upper limit of 14 Å on the range of wavelengths that can be used, limiting the

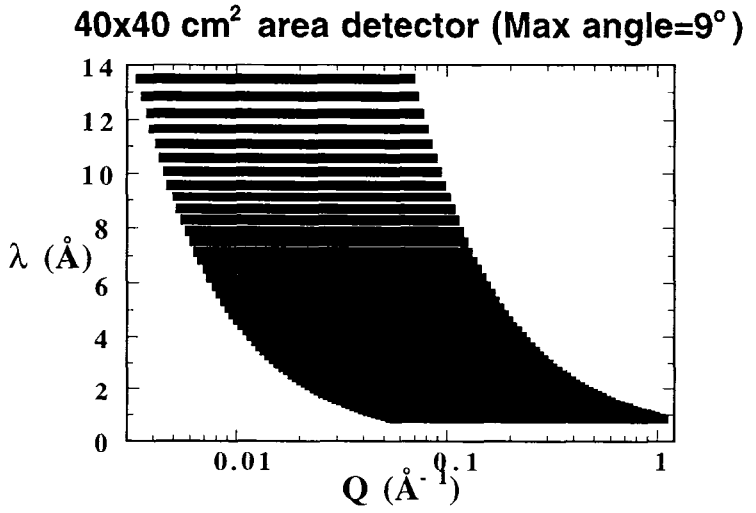

Figure 5. The Q-range at different wavelengths at SAND.

Q_{min} that can be reached. However, if the chopper revolves at 7.5 Hz so that the beam is opened at 15 Hz, the chopper blocks every second pulse. By increasing the separation in time between neutron pulses, the upper limit on the useable wavelength can be increased to 28 Å, and that will decrease the Q_{min} value by half. At the same time, the chopper continues to remove a substantial fraction of the delayed neutrons from the beam. At present we are working to stabilize the phasing between the chopper and the neutron pulses so that the chopper can run at 7.5 Hz as well as at the current 15 Hz. In addition we plan to employ high resolution Soller collimators and a high resolution 40 x 40 cm^2 area sensitive proportional counter to extend the Q_{min} to 0.002 $Å^{-1}$ using λ_{max} = 14 Å.

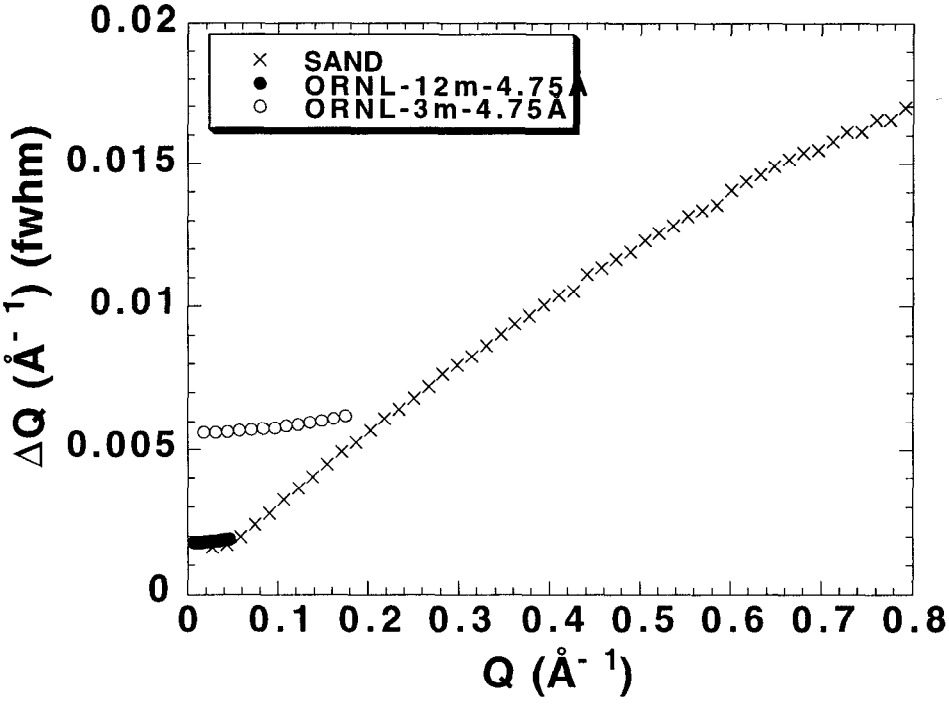

Figure 6. The Q resolution of SAND and the SANS instrument at ORNL.

To extend the Q_{max} to higher values we have already installed a bank of linear position sensitive detectors. Implementation to produce data in the higher Q region is in progress. We have shown the Q-range accessed by the 40 x 40 cm^2 area detector at different wavelengths in Fig. 5. The maximum scattering angle subtended by the high-angle bank of detectors will increase from 9° to 36°, not only extending the Q-range on the high Q side but also improving the quality of the data in the whole Q region. In the low Q region the ΔQ resolution of SAND is comparable to that at the reactor-based instruments, while at the higher Q region the resolution of SAND is superior (see Fig. 6).

SAND has a variety of ancillary equipment such as furnaces, a sample changer, a pressure cell, and a shear cell (Table II) for controlling the sample environment.

Table II. Ancillary Equipment Available at SAND

Equipment	Environment	Temperature Range
10 Position Sample Changer (circulating bath)	Ambient, Nitrogen Purge	10 – 90°C
Resistance Heater	Ambient, Coarse vacuum, Nitrogen Purge	30 - 250°C
1 - 60 rps Shear Cell	Ambient	10 - 90°C
Furnace (under development)	Vacuum	100 - 1700°C
Displex	High vacuum	5 - 300 K
Sample Stretcher (elastomer films)	Ambient	Ambient
Sample Rotator (slurry, suspensions)	Ambient, Nitrogen purge	Ambient
Pressure Cell (liquid samples)	1-2500 bars	0 – 80°C
Magnet	5 to 10 K Gauss	

3. Standard Samples

In our previous paper [1] we have shown that the quality of the SANS data from SAD is comparable to that from the reactor-based SANS instruments. When the data are measured in a wide Q region, the experiment times are comparable even with the high-power reactor-based instruments. SAND surpasses SAD in both the Q-range and in the statistical precision of the data. In order to show that the quality of the data from SAND is comparable to that from the reactor-based SANS instruments, we have shown data for the Bates-poly standard in Fig.4 and for the vycor glass sample in Fig. 7. As can be

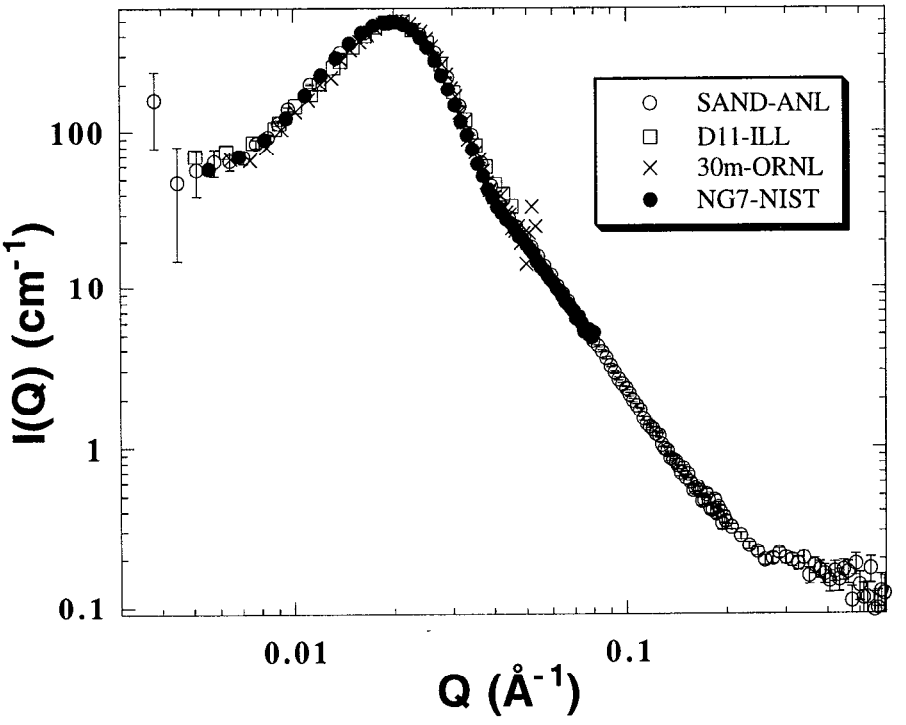

Figure 7. SANS data measured at various centers for Vycor glass.

seen from the figures, the data measured at reactor-based SANS instruments at two settings cover only approximately half of the Q-range covered by SAND in a single measurement. Moreover, scattering data in a wide Q region is required to properly characterize the nanostructure of the pores and their spatial correlation in this type of glass.

4. Scientific Examples

The wide Q region available at SAND in a single measurement is very important for a number of problems, especially for studies involving systems that may change as a function of time and other experimental conditions. This is especially true for studying samples at extreme conditions such as high temperature, pressure and shear. Here we give two examples that took advantage of the Q-range accessed by SAND.

4.1. Stability of Chaperonin from *S. shibatae*

The first system deals with the structure of a supramolecular protein complex of the major heat shock protein from *S. shibatae* [7] at different temperatures as a function of cofactors ATP and Mg. In this organism the chaperonin proteins, with MW of about 57

kD, self-assemble to form a 18-mer supramolecular complex which resembles a double-doughnut structure. SANS study of a similar system from *E. coli* has clearly shown that the double-doughnut structure produces peaks in the scattering data [8]. The self-assembled supramolecular protein structure from *S. shibatae* also produces several secondary peaks in the SANS pattern as in Fig. 8. If the protein monomers formed random aggregates, they would not produce such secondary peaks. The 18-mer complex is believed to provide protection to the organism's other proteins that may denature under stress such as high temperature. According to biochemical studies, the self-assembly process as well as the stability of the 18-mer complex depends on the presence of ATP and Mg. In the absence of ATP and Mg the complex aggregates at elevated temperatures. Elucidating the structural features that evolve at different temperatures as a function of cofactors will require data in a wide Q region. The low Q data is essential to determine the molecular weight of the complex as well as to determine whether any larger

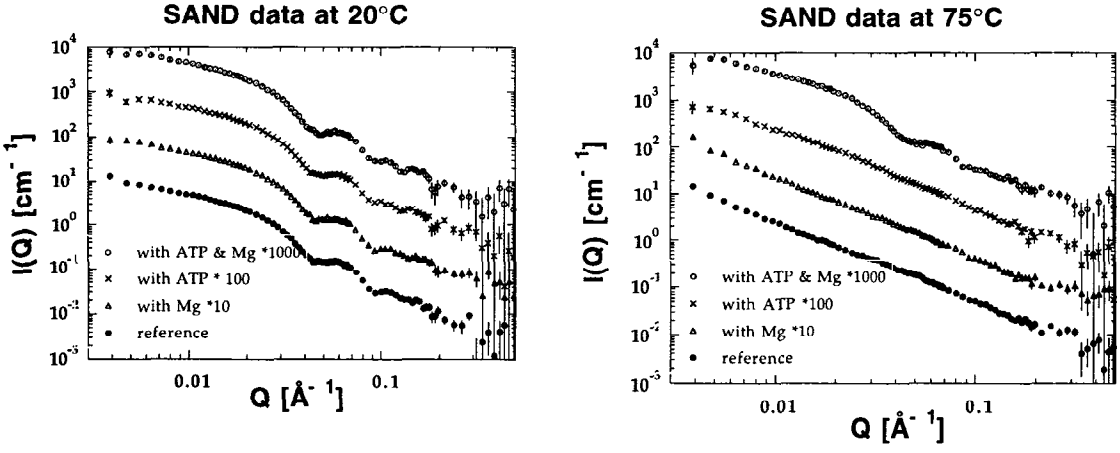

Figure 8. SANS of Chaperonin from *S. shibatae* in D_2O from SAND.

complexes are formed. The high Q data (secondary peaks) is required to infer the presence and stability of the 18-mer complex. This complex system thus requires data in a wide Q region, preferably measured in a single measurement as these are delicate and may slowly change with time even during storage. To elucidate the structural features in this system we measured the protein samples in D_2O solution at different temperatures at SAND. In Fig.8 we have shown the data at 20°C and 75°C. The presence of the18-mer complex is clearly seen at all conditions at 20°C. However, at 75°C the complex is stable only in the presence of both ATP and Mg. In the absence of either of those cofactors the proteins seem to form tubules through end-to-end association. Since Q_{min} at SAND is

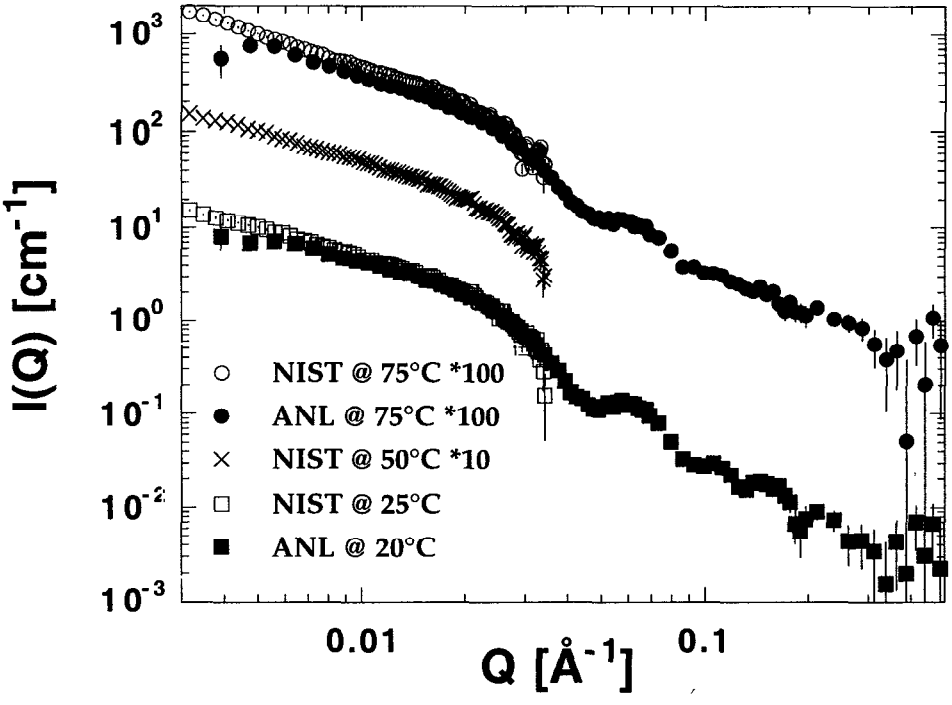

Figure 9. SANS of chaperonin from *S. shibatae*+ATP+Mg in solution at different temperatures from SAND at ANL and NG3 at NIST.

limited, we measured this system in the low Q region at the SANS instrument at NIST. In Fig. 9 we have compared the NIST data with that from SAND. The data sets agree well in regions where data overlap. The low Q data from NIST indicate that the particles are quite larger; however, the Q-range spanned in a single measurement at NG3-SANS is insufficient to determine whether the particles are indeed polymers of the 18-mer complex or precipitates. On the other hand, the Q_{min} at SAND is inadequate for the complete characterization of the system. The best situation would be to have a TOF-SANS instrument that can cover a wide Q region of 0.002 to 2 Å^{-1} in a single measurement. We plan to improve SAND to accomplish that.

4.2 Environmentally Responsive Gels

Our second example is environmentally responsive gel samples provided by Prof. S. Gehrke, University of Cincinnati. We measured hydrogels of hydroxypropyl cellulose (HPC) and poly(N-isopropylacrylamide) (PNIPAAm) in D_2O that undergo similar shrinking when heated above their respective transition temperatures, but exhibit quite different permeabilities [9]. This suggests that the internal structure of the collapsed state of HPC hydrogel is quite different from that of PNIPAAm gels. Understanding this highly unusual behavior is of significant practical and fundamental importance, as gels

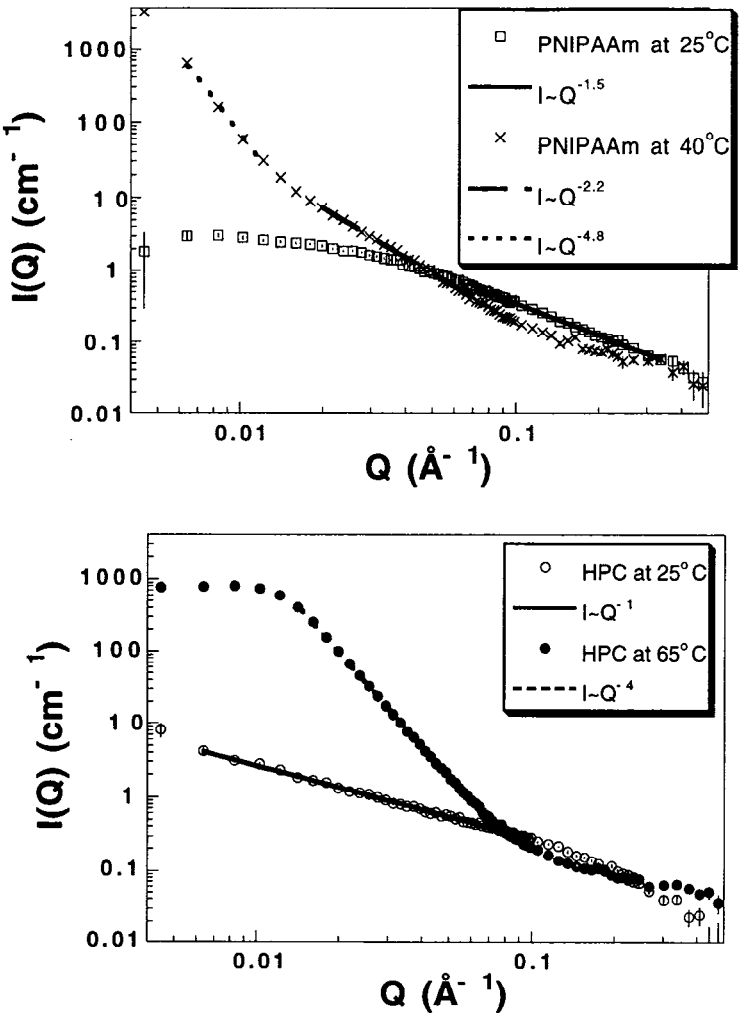

Figure 10. SANS data and suggested structure of PNIPAAm and HPC hydrogel at room temperature and above their respective transition temperatures.

are widely used in separation media and biomedical applications, e.g. chromatography, gel electrophoresis, artificial organs, and drug delivery. The wide Q-range monitored in a single experiment on SAND was very important for this study because the shrinking process follows complicated kinetics, and it was not clear from the beginning on what length scales the most dramatic structural differences would be observed. Our experimental data (Fig. 10) illustrate that this problem requires data in a wide Q-range in a single measurement.

The SANS from PNIPAAm at 25°C shows a power law scattering of $Q^{-1.5}$ and a plateau region at lower Q. We observe the scattering of network strands that are not fully stretched (Q^{-1}) but rather follow the self-avoiding path of linear polymers in a good solvent ($Q^{-5/3}$). At $Q < 0.05$ Å^{-1} the network strand correlation vanishes, as the observed length scale exceeds the network mesh size and the gel appears homogenous. Upon

heating above its transition temperature, PNIPAAm reveals a gradual change of structure in the high Q data. The observed exponent close to -2 suggests a random coil structure of network strands. We believe that D_2O is trapped in the network, giving rise to the huge increase in scattering intensity at $Q < 0.01$ Å^{-1}. The large exponent of -4.8 in the power law scattering indicates a diffuse surface of the solvent filled cavities, which is very likely due to a swelling gradient across the D_2O/collapsed-gel interface. The scattering patterns of HPC are very different. At room temperature stretched network strands (Q^{-1}) are observed. Upon heating above its transition temperature, HPC forms 3-dimensional objects with smooth surface (Q^{-4}). Since the collapsed hydrogel contains comparable volumes of HPC and D_2O, it is difficult to conclude further on the nature of these objects, i.e. whether we see HPC agglomerates in D_2O or D_2O-filled pores in HPC matrix or a mix of both. A more thorough analysis is in progress.

5. Summary

The performance of the SAND instrument is comparable to that of reactor-based instruments over the full range of Q available. Measurements of scattering by standard samples at SAND have demonstrated that data measured at SAND is similar in quality to that measured in comparable times at instruments at the most powerful research reactors. Furthermore, the ΔQ resolution of the SAND instrument is the same or better than that of the reactor-based instruments. Work is currently underway to improve the versatility and ease of operation and the quality of the data measured with SAND. The new high-angle bank of linear position-sensitive detectors will increase the maximum Q accessible to 2 Å^{-1} and increase the quality of data in the high Q region. Similarly, the range and quality of the data measured at low Q will be improved through the installation of finer focussing soller collimators and a higher resolution area detector and through the implementation of a frame-elimination mode for the delayed-neutron chopper. The wide Q-range accessible in a single measurement allows for the simultaneous measurement of local structure, molecular weight, and aggregation of subunits from a single sample. This is a great advantage for parametric studies and measurements involving delicate systems or samples that are annealing, organizing, or otherwise evolving in time.

Acknowledgment

The authors acknowledge the valuable contributions of Dr. J. E. Epperson and R. Kleb in the design and building of SAND instrument. We also thank our collaborators Dr. Joachimiak, CMB Division, Argonne National Laboratory, and Dr. S. Gehrke, University of Cincinnati, for permitting us to use the data in the scientific examples.

References

[1] P. Thiyagarajan, J. E. Epperson, R. K. Crawford, J. M. Carpenter, T.E. Klippert and D. G. Wozniak, The Time-of-Flight Small Angle Neutron Diffractometer (SAD) at IPNS, Argonne National Laboratory, *J. Appl. Cryst.*, , 30, 280-293, 1997.

[2] R. K. Crawford, P. Thiyagarajan, J. E. Epperson, F. Trouw, R. Kleb, D. Wozniak and D. Leach, The New Small-Angle Diffractometer SAND at IPNS. *Proc. 13th International Collaboration on Advanced Neutron Sources, Switzerland,* October 11-14, 1995, *PSI-Proc* 95-02, 99-117, 1996.

[3] P. Thiyagarajan, D. Mildner and R.K. Crawford, Neutron Transmission of a Single Crystal Mgo Filter J. Apply. Cryst, 1998 (In Press).

[4] R. K. Crawford, J. E. Epperson, P. Thiyagarajan and J. M. Carpenter, Analysis of a Drum Chopper for Use on a New Small Angle Diffractometer at IPNS. Proc. ICANS-XI 873-889, 1990.

[5] J. E. Epperson, J. M. Carpenter, P. Thiyagarajan, and B. Heuser, Measurement of the Delayed Neutron Fraction and Correction of Small Angle Scattering Data from a Pulsed Spallation Source for This Effect, Nuclear Instruments and Methods A289, 30-34, 1990.

[6] R.K. Crawford, J.E. Epperson and P. Thiyagarajan, Soller Collimators for Small-Angle Neutron Scattering, Inst. Phys. Ccof. Ser. (97) 419-426, 1989.

[7] B.M. Phipps et al., Structure of a molecular chaperone from a thermophiclic archaebacterium, Nature, 361, 475-477, 1993.

[8] P. Thiyagarajan, S.J. Henderson and A. Joachimiak, Solution structures of GroEL and its complex with rhodanese from small-angle neutron scattering, Structure 4, 79-88, 1996.

[9] S. Gehrke in Responsive Gels: Volume Transitions II, 81-144, Springer-Verlag, Berlin, New York, 1993.